Article

Optimization and Antibacterial Evaluation of Novel 3-(5-Fluoropyridine-3-yl)-2-oxazolidinone Derivatives Containing a Pyrimidine Substituted Piperazine

Xin Wang [1], Bo Jin [1], Yutong Han [1], Tong Wang [1], Zunlai Sheng [1,2], Ye Tao [1,2] and Hongliang Yang [1,2,*]

[1] Department of Veterinary Medicine, Northeast Agricultural University, Harbin 150030, China
[2] Heilongjiang Key Laboratory for Animal Disease Control and Pharmaceutical Development, Harbin 150030, China
* Correspondence: hongl_yang@126.com

Abstract: In this study, a series of novel 3-(5-fluoropyridine-3-yl)-2-oxazolidinone derivatives were designed and synthesized based on compounds previously reported, and their antibacterial activity was investigated. Then their antibacterial activity was investigated for the first time. Preliminary screening results showed that all these compounds exhibited antibacterial activity against gram-positive bacteria, including 7 drug-sensitive strains and 4 drug-resistant strains, among which compound **7j** exhibited an 8-fold stronger inhibitory effect than linezolid, with a minimum inhibitory concentration (MIC) value of 0.25 μg/mL. Further molecular docking studies predicted the possible binding mode between active compound **7j** and the target. Interestingly, these compounds could not only hamper the formation of biofilms, but also have better safety, as confirmed by cytotoxicity experiments. All these results indicate that these 3-(5-fluoropyridine-3-yl)-2-oxazolidinone derivatives have the potential to be developed into novel candidates for the treatment of gram-positive bacterial infections.

Keywords: 3-(5-fluoropyridine-3-yl)-2-oxazolidinone derivatives; antibacterial activity; molecular docking; antibiofilm activity; drug resistance

1. Introduction

Bacterial infections can lead to skin suppuration, bacteremia, local and systemic inflammation, and other serious diseases [1]. With the discovery and development of antibiotics, revolutionary changes have taken place in the treatment of bacterial infections, effectively reducing infection rates and mortality. However, the irregular use of antimicrobial drugs has led to the emergence of various drug-resistant strains, which are considered dangerous and stubborn clinical pathogens that cause difficult-to-treat, life-threatening illnesses [2]. Furthermore, it has been found in clinical studies that many pathogenic bacteria can adhere to the surfaces of objects, secrete metabolites, and generate extracellular polymeric substances (EPS), thus forming biofilms with a "cell population-metabolite" structure, which can effectively protect strains and produce drug resistance, leading to a high incidence of nosocomial infection and a high treatment cost [3,4]. Although great efforts have been made to create novel and effective antimicrobial methods, the pace of development is too slow to meet clinical needs [5–8].

At present, many pharmaceutical chemists are trying to develop new antibacterial drugs with novel structures, unique mechanisms of action, and long-term effectiveness [9–11]. Oxazolidinones are a class of chemosynthetic antibacterial drugs with a brand-new chemical structure, similar to sulfonamides and quinolones, which are used to treat skin and tissue infections, pneumonia, untreatable bacterial infections, and other infectious diseases caused by gram-positive bacteria [12]. Oxazolidinones have been widely used and studied because of their unique antibacterial mechanism, that is, inhibition of protein synthesis at the initial stage and no cross-resistance with other antibacterial drugs [13–16]. Moreover, some oxazolidinone analogues have been marketed previously [17–19]. Although the initial effect is satisfactory,

drug resistance appears after long-term use, accompanied by thrombocytopenia and other adverse reactions [20]. This has prompted pharmaceutical chemists to continue to improve oxazolidinone antimicrobials with higher antimicrobial activity and sustained sensitivity [21–29].

Our research group previously modified the structure of linezolid (Figure 1) [30–34], found that compounds **1** and **2** have efficient antibacterial activity for *S. aureus*, *Streptococcus pneumoniae*, *Enterococcus faecalis*, etc. (MICs = 4~64 µg/mL) and exciting antibiofilm activity (MBIC = 0.5~8 µg/mL). The vinyl structure in these molecules is retained and cyclized to form a new aromatic heterocyclic ring. Considering the unique electronegativity of pyrimidines and their ability to form hydrogen bonds [35], pyrimidine aromatic rings were introduced into the structure [36]. Accordingly, a series of 3-(5-fluoropyridine-3-yl)-2-oxazolidinone derivatives were synthesized and tested for antibacterial activity (Figure 2).
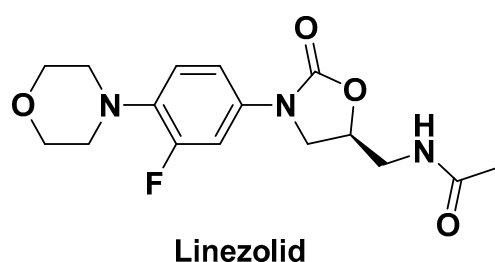
Figure 1. The structure of linezolid.
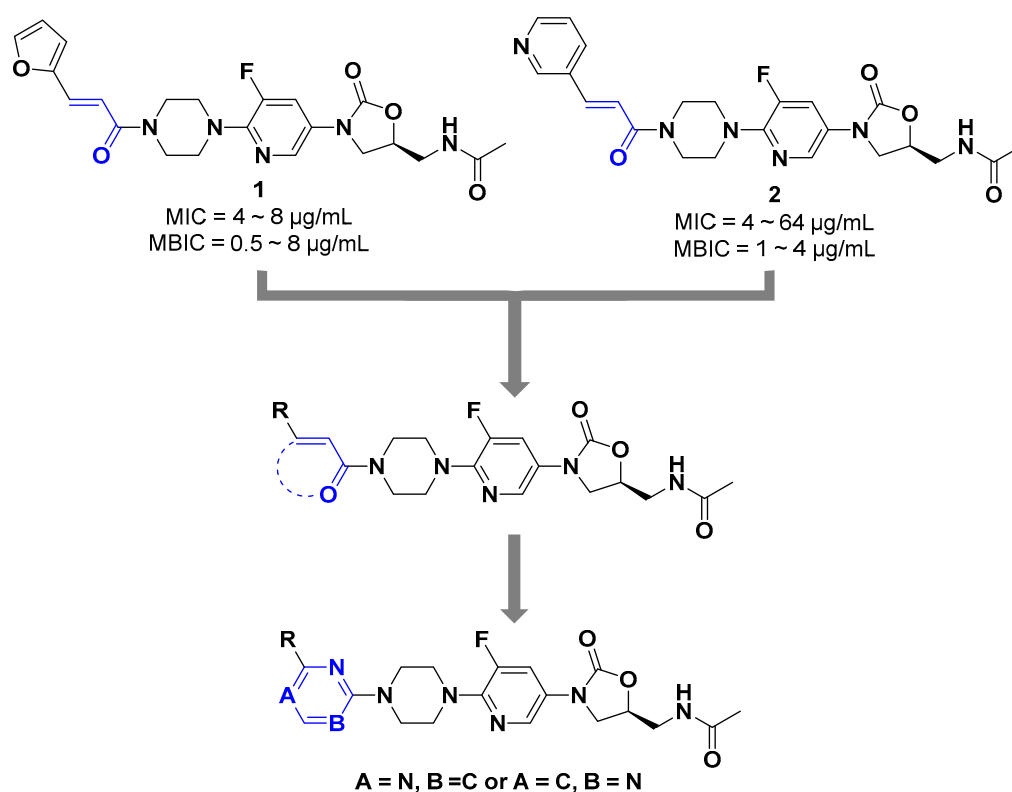
Figure 2. Optimization strategy of novel oxazolidinone derivatives.

2. Results and Discussion

2.1. Chemistry

According to the steps described in the literature [37], intermediate **4** was produced through a multi-step reaction by commercially purchased compound **3**. After removing the Boc protection group, compound **4** was coupled with 2,4-dichloropyrimidine to produce intermediate **5**. The intermediate **5** was linked with different amines to generate the final

products **6a-m**, as displayed in Scheme 1. Furthermore, the final products **7a-n** were obtained by a similar method.
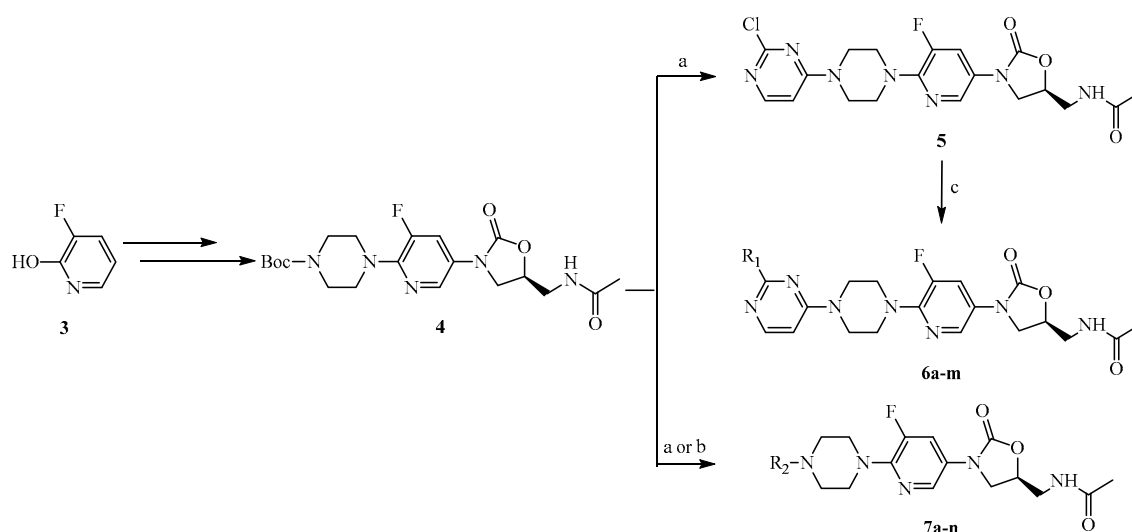
Reagents and conditions: (a) (1) TFA, DCM, 0 °C, 2 h; (2) pyrimidine, TEA, dioxane, rt, overnight; (b) (1) TFA, DCM, 0 °C, 2 h; (2) pyrimidine, TsOH, amine, EtOH, overnight; (c) TsOH, amine, EtOH, overnight.

Scheme 1. Synthesis of target compounds **5**, **6a-m** and **7a-n**.

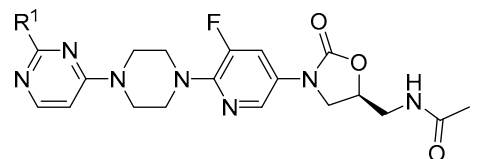### 2.2. Antibacterial Activity Assay

2.2.1. Minimum Inhibitory Concentration against Standard Strains
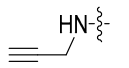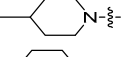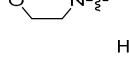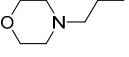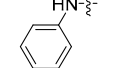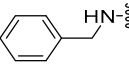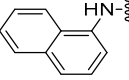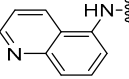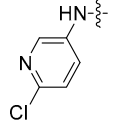
Intermediate **5** and further derivatives **6a-m** were synthesized and tested against a panel of gram-positive bacteria using the double dilution method. As shown in Table 1, all these compounds had moderate antibacterial activity against all six tested gram-positive bacteria but no activity against gram-negative bacteria (*E. coli*). The MICs of compounds **6a-m** were 2~32 µg/mL against gram-positive bacteria, while the MIC was 1~2 µg/mL when R^1 = Cl (**5**), which had better antibacterial activity. It was speculated that the cavity of the target near the R^1 side chain was not large enough for these substituent groups.

Table 1. The MICs (µg/mL) of compounds **5**, **6a-m** against 7 standard strains. (MIC: minimal inhibit concentration).

Compound	R^1	Sa [a]	Sp [b]	Ef [c]	Bs [d]	Sx [e]	Lm [f]	Ec [g]
5	-Cl	1	1	1	1	1	2	>128
6a	HN-	8	16	8	8	8	32	>128
6b	HN-	16	16	16	16	8	16	>128
6c	HN-	8	8	8	8	8	8	>128
6d	HN-	8	8	8	4	8	32	>128
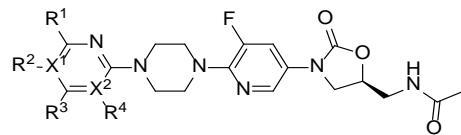
Table 1. *Cont.*

Compound	R^1	Sa [a]	Sp [b]	Ef [c]	Bs [d]	Sx [e]	Lm [f]	Ec [g]
6e		8	8	16	8	16	64	>128
6f		16	32	32	32	16	128	>128
6g		16	16	16	16	16	32	>128
6h		8	8	8	8	8	16	>128
6i		8	16	8	8	8	64	>128
6j		8	8	8	8	8	16	>128
6k		32	16	32	32	8	32	>128
6l		8	8	8	8	8	16	>128
6m		2	2	8	4	4	32	>128
linezolid	-	2	2	2	2	2	2	>128

[a] Sa, *Staphylococcus aureus* (ATCC25923); [b] Sp, *Streptococcus pneumoniae* (ATCC49619); [c] Ef, *Enterococcus faecalis* (ATCC29212); [d] Bs, *Bacillus subtilis* (ATCC6633); [e] Sx, *Staphylococcus xylosus* (ATCC35924); [f] Lm, *Listeria monocytogenes* (ATCC19111); [g] Ec, *Escherichia coli* (ATCC25922).

After that, a series of pyrimidine derivatives, **7a-n** without a further substituted group, was synthesized, and their antibacterial activity was tested (Table 2). All these compounds, except **7m**, had better antibacterial activity than compounds **1** and **2**, but these compounds still exhibited no effect against gram-negative bacteria. Among them, compound **7j** exhibited the best activity with a MIC of 0.25~1 μg/mL. First, while keeping X^1 = N, three substituent groups on the pyrimidine ring (R^1 = Cl, NH$_2$, or R^1 = R^3 = Cl) were examined (**5**, **7e** and **7h**). All of them exhibited better activities than the compounds with X^1 = C (**7b**, **7f** and **7g**). Then, by comparing the activity of chlorine-substituted compounds **5**, **7a**, **7h**, **7j** and **7n**, it was found that the number of chlorine atoms had no significant influence on activity. Meanwhile, keeping X^1, X^2, R^1, and R^3 constant (X^1 = N, X^2 = C, R^1 = Cl, and R^3 = H), F, Cl, Br, and methyl substituent groups on R^4 were examined. All these derivatives displayed similar biological activities (MICs = 0.25~4 μg/mL), indicating that F, Cl, Br, or methyl were acceptable as substituents.

Table 2. MICs (µg/mL) of compounds **7a-n** against 7 standard bacteria. (MIC: minimal inhibit concentration).

Compound	X^1	X^2	R^1	R^2	R^3	R^4	Sa [a]	Sp [b]	Ef [c]	Bs [d]	Sx [e]	Lm [f]	Ec [g]
7a	N	C	H	-	Cl	H	2	4	2	2	2	2	>128
7b	C	N	Cl	H	H	-	2	1	2	2	2	8	>128
7c	C	N	H	CH₃	H	-	2	2	4	2	1	1	>128
7d	C	N	H	Br	H	-	2	4	2	4	2	2	>128
7e	N	C	NH₂	-	H	H	0.5	0.5	1	1	1	0.5	>128
7f	C	N	NH₂	H	H	-	2	1	1	1	2	4	>128
7g	C	N	Cl	H	Cl	-	2	4	8	16	2	2	>128
7h	N	C	Cl	-	Cl	H	2	2	1	2	1	2	>128
7i	N	C	Cl	-	H	F	0.5	0.5	1	1	1	0.5	>128
7j	N	C	Cl	-	H	Cl	1	0.25	1	1	1	0.25	>128
7k	N	C	Cl	-	H	Br	1	0.5	0.5	1	2	0.5	>128
7l	N	C	Cl	-	H	CH₃	0.5	1	4	4	2	0.5	>128
7m	N	C	CH₃S	-	H	C₂H₅OCO	32	32	32	32	32	32	>128
7n	N	C	Cl	-	Cl	Cl	2	4	2	2	2	2	>128
linezolid	-	-	-	-	-	-	2	2	2	2	2	2	>128

[a] Sa, *Staphylococcus aureus* (ATCC25923); [b] Sp, *Streptococcus pneumoniae* (ATCC49619); [c] Ef, *Enterococcus faecalis* (ATCC29212); [d] Bs, *Bacillus subtilis* (ATCC6633); [e] Sx, *Staphylococcus xylosus* (ATCC35924); [f] Lm, *Listeria monocytogenes* (ATCC19111); [g] Ec, *Escherichia coli* (ATCC25922).

2.2.2. Minimum Inhibitory Concentration against Drug-Resistant Strains

After evaluating the antibacterial potential of these derivatives, they were further tested against clinically isolated resistant bacteria. As shown in Table 3, these MIC results show that compounds **7i-l** had significant antibacterial activity against MRSA and VRE but no effect against linezolid-resistant strains.

Table 3. The MICs (µg/mL) of compounds **7i-l** against four drug-resistance bacteria. (MIC: minimal inhibit concentration).

Compound	MRSA [a]	VRE [b]	LRSA [c]	LRSP [d]
7i	1	1	>128	>128
7j	1	1	>128	>128
7k	1	1	>128	>128
7l	1	1	>128	>128
linezolid	2	2	>128	>128

[a] MRSA, Methicillin-resistant *Staphylococcus aureus*; [b] VRE, Vancomycin-resistant *Enterococcus*; [c] LRSA, Linezolid-resistant *Staphylococcus aureus*; [d] LRSP, Linezolid-resistant *Streptococcus pneumoniae*.

2.3. Molecular Docking Study

To understand binding site, state, conformation, and interaction, the promising compound **7j** was selected for further docking study with the 50S ribosomal subunit from *Haloarcula Marismortui* (PDB ID: 3CPW) [38,39]. As shown in Figure 2, the compound that expanded linearly bound to the peptidyl transferase center (PTC) of the 50S ribosomal subunit. The potential compound existed in the cavity of PTC, which was composed by U2619, U2540, G2539, U2583, U2538, C2486, G2101, and A2485. Moreover, the H atom and O atom on the 5-side chain amide group of the oxazolidinone ring formed a hydrogen bond with A2485 and A2636, respectively. In addition, the pyrimidine ring of compound **7j** and the pyrimidine ring formed π-π conjugations with C2486 and U2538.

As can be seen from Figure 3, the 2-Cl atom on the pyrimidine substituent extended into a shallow pocket, which was too small to accommodate other groups on the pyrimidine. That was probably the reason why compounds **6a-m** had worse antibacterial activity.

Meanwhile, there was a larger space between the 5-Cl atom on the pyrimidine substituent and the surface of the cavity, which might be the reason why compounds **7i-m** had a better antibacterial effect.
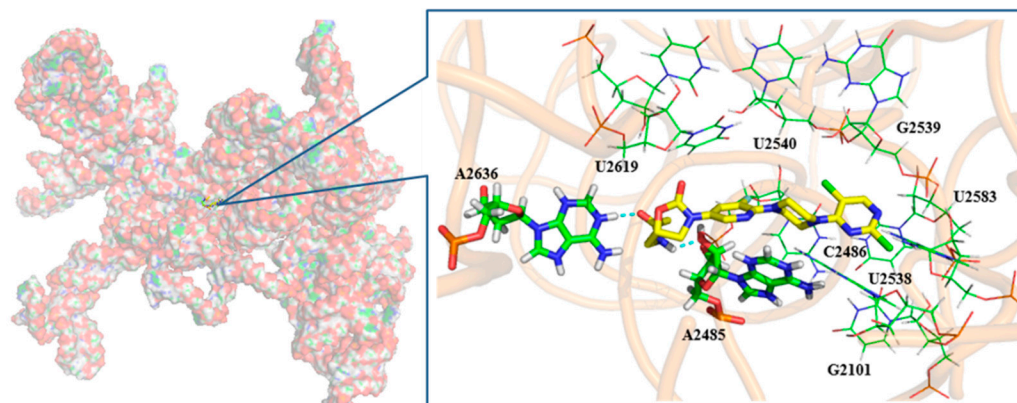

Figure 3. Docking results for **7j** with the 50S ribosomal subunit from *Haloarcula Marismortui* (PDB ID: 3CPW). The O atom (red), the N atom (blue), and the C atom (yellow) are shown. Hydrogen bonds are shown as dashed green lines.

2.4. Inhibition of Biofilm Formation

Using the microtiter dish biofilm formation assay [40], four potent compounds were selected for further evaluation of their effects on bacterial biofilm formation against four drug-resistant strains. As shown in Table 4, the results show that all these compounds significantly inhibited the formation of biofilms, with the minimum biofilm inhibitory concentrations (MBICs) of 0.5 µg/mL against MRSA and VRE and 1~4 µg/mL against LRSA and LRSP. The above results indicate that these compounds can significantly inhibit the growth of biofilm, and it could be speculated that they have stable effects and do not easily develop resistance to bacteria. Meanwhile, the results show that all compounds are more effective than linezolid against four drug-resistant strains, which indicates all compounds have different mechanisms with linezolid.

Table 4. MBICs (µg/mL) of compounds **7i-l** against 4 drug-resistant bacteria.

Compound	MRSA [a]	VRE [b]	LRSA [c]	LRSP [d]
7i	0.5	0.5	2	4
7j	0.5	0.5	1	4
7k	0.5	0.5	1	4
7l	0.5	0.5	2	4
Linezolid	64	16	128	128

[a] MRSA, Methicillin-resistant *Staphylococcus aureus*; [b] VRE, Vancomycin-resistant *Enterococcus*; [c] LRSA, Linezolid-resistant *Staphylococcus aureus*; [d] LRSP, Linezolid-resistant *Streptococcus pneumoniae*.

2.5. Cytotoxicity Determination

When a chemical substance is used to treat infection, it may affect the physiological activity of both cells and bacteria, thereby reducing the cell's survival rate [41]. Therefore, it was necessary to evaluate the toxicity of active derivatives. The cytotoxicity of compound **7j** against the Hela cell line was detected via the MTT colorimetric assay, as shown in Table 5. The result shows that the cytotoxicity of the tested compound increased in a dose-dependent manner, and cell survival at 256 µg/mL and lower concentrations was higher than 85%. Considering that the cytotoxicity only appeared above 256 µg/mL, which was 64~512 times that of its MICs. Consequently, the compound **7j** has the potential to be further developed as an antibacterial drug.

Table 5. Analyzing the toxicity of compound **7j** against human cervical-cancer cells (Hela) using the MTT assay.

Concentration (μg/mL)	32	64	128	256	500	1000
cell viability (%)	100	97.5	96.9	93.5	33.3	7.3

3. Experimental Section

3.1. Materials and Methods

All the chemicals and solvents used in this study were of analytical grade. All the reagents were purchased from Tianjin Tianli Chemical Reagent Co., Ltd., Tianjin, China. All solvents and chemicals were purified by standard methods. Unless otherwise stated, the synthesis of all compounds was monitored by thin layer chromatography (TLC) and purified by rapid column chromatography. Thin layer chromatography (TLC) was performed on silica gel G plates (Taizhou Luqiao Sijia Biochemical Plastic Products Factory, Taizhou, China). The melting point (m. p.) of all products was measured by the SGW X-4A micro-melting point meter apparatus. All compounds were tested to verify their purity by HPLC (Shimadzu Corporation, Kyoto, Japan). Using the Diamonsil C18 column, the mobile phase was acetonitrile and water of different gradients at a flow rate of 1.0 mL•min^{-1}. The column temperature was set at 35 °C and the injection volume of each sample was 10 μL. Every sample was quantitatively diluted with methanol to 1 mg•mL^{-1}. ^{1}H NMR spectra (600 MHz) and ^{13}C NMR spectra (150 MHz) were recorded on a Bruker Advance spectrometer with tetramethyl-silane (TMS) as the internal standard and DMSO-d_6 as the solvent. The used standard strains were purchased from the American Type Culture Collection (ATCC), and the drug-resistant strains were isolated from clinical sources. The Hela cells were donated by Dr. Tao Wang (Qiqihar Medical University).

3.2. Chemistry

3.2.1. Synthesis of (S)-N-((3-(6-(4-(2-chloropyrimidin-4-yl)piperazin-1-yl)-5-fluoropyridin-3-yl)-2-oxooxazolidin-5-yl)methyl)acetamide(5)and(S)-N-((3-(6-(4-(4-chloropyrimidin-2-yl)piperazin-1-yl)-5-fluoropyridin-3-yl)-2-oxooxazolidin-5-yl)methyl)acetamide (**7b**)

A solution of compound **4** (218 mg, 0.5 mmol) in DCM (5 mL) at 0 °C was dropwise added to TFA (1 mL) and then stirred for 2 h. After the reaction was complete, TEA was added to the solution at 0 °C to adjust pH. The filtrate was concentrated in vacuo. To a solution of the concentrate in ethanol (3 mL) was added TEA (0.14 mL, 1 mmol) and 2, 4-dichloropyrimidine (97 mg, 0.65 mmol), and then stirred at reflux overnight. After the reaction was complete and concentrated, the mixture was extracted with DCM (5 mL × 3). The organic phase was washed with brine and concentrated in vacuo. The residue was purified by silica gel column chromatography (DCM/MeOH/TEA = 50:1:1) to yield compounds **5** and **7b**.

Compound **5** was white solid; yield 5.8%. m. p. 171.1–173.1 °C. ^{1}H NMR (600 MHz, DMSO-d_6) δ 8.32 (t, J = 6.0 Hz, 1H), 8.14 (d, J = 2.4 Hz, 1H), 8.11 (d, J = 6.0 Hz, 1H), 7.94 (dd, J = 14.4, 2.4 Hz, 1H), 6.88 (d, J = 6.0 Hz, 1H), 4.79 − 4.72 (m, 1H), 4.13 − 4.10 (m, 1H), 3.79 − 3.72 (m, 5H), 3.46 − 3.40 (m, 6H), 1.84 (s, 3H). ^{13}C NMR (150 MHz, DMSO-d_6) δ 170.6, 163.0, 160.0, 158.0, 154.8, 149.1 (d, JC-F = 257.1 Hz), 145.6, 133.0, 130.0, 115.4, 102.9, 72.6, 55.4, 47.6, 47.4, 41.9, 22.9. HRMS (ESI) (positive mode) *m/z* calculated for $C_{19}H_{21}ClFN_7O_3$: 449.87; Found: 450.129.

Compound **7b** was white solid; yield 40.4%. m. p. 160.0–161.1 °C. 1H NMR (600 MHz, DMSO-d6) δ 8.35 (d, J = 5.4 Hz, 1H), 8.25 (t, J = 6.0 Hz, 1H), 8.13 (d, J = 2.4 Hz, 1H), 7.93 (dd, J = 14.4, 2.4 Hz, 1H), 6.77 (d, J = 5.4 Hz, 1H), 4.89 − 4.63 (m, 1H), 4.21 − 4.02 (m, 1H), 3.82 − 3.79 (m, 4H), 3.75 − 3.67 (m, 1H), 3.44–3.33 (m, 5H), 1.84 (s, 3H). ^{13}C NMR (150 MHz, DMSO-d_6) δ 170.5, 161.5, 160.5, 154.8, 149.1 (d, JC-F = 257.1 Hz), 145.9, 133.0, 130.0, 128.7, 115.4, 109.7, 72.6, 47.7, 46.1, 43.7, 41.9, 22.9. HRMS (ESI) (positive mode) *m/z* calculated for $C_{19}H_{21}ClFN_7O_3$: 449.87; Found: 450.119.

Raw data for the above products are presented in Supplementary Materials (Figures S1–S3 and S46–S48).

3.2.2. General Procedure for the Synthesis of **6a** and **6b**

A solution of compound **5** (200 mg, 0.44 mmol) in an amine solution (4 mL) was stirred at room temperature for three days. After the reaction was complete, the filtrate was concentrated in vacuo. The mixture was extracted with DCM (5 mL × 3). The organic phase was washed with brine and concentrated in vacuo. The residue was purified by silica gel column chromatography (DCM/MeOH = 30:1) to yield compounds **6a** and **6b**.

*(S)-N-((3-(5-fluoro-6-(4-(2-(methylamino)pyrimidin-4-yl)piperazin-1-yl)pyridin-3-yl)-2-oxooxazolidin-5-yl)methyl)acetamide (**6a**).*

Compound **6a** was a yellow solid; yield 40.5%. m. p. 193.3–195.1 °C. ^{1}H NMR (600 MHz, DMSO-d_6) δ 8.27 (t, J = 6.0 Hz, 1H), 8.14 (d, J = 2.4 Hz, 1H), 7.94 (dd, J = 14.4, 2.4 Hz, 1H), 7.86 (d, J = 6.6 Hz, 1H), 7.31 − 7.30 (s, 1H), 6.31 (d, J = 6.6 Hz, 1H), 4.78 − 4.73 (m, 1H), 4.13 − 4.10 (m, 1H), 3.84 − 3.78 (s, 4H), 3.75 − 3.73 (m, 1H), 3.43 − 3.42 (m, 6H), 2.82 (d, J = 4.8 Hz, 3H), 1.84 (s, 3H).^{13}C NMR (150 MHz, DMSO-d_6) δ 170.5, 162.0, 154.8, 149.1 (d, JC-F = 257.1 Hz), 145.7, 145.7, 133.0, 133.0, 130.0, 115.6, 115.5, 72.6, 47.7, 47.6, 43.9, 41.9, 28.1, 22.9. HRMS (ESI) (positive mode) m/z calculated for $C_{20}H_{25}FN_8O_3$: 444.47; Found: 445.150.

(S)-N-((3-(5-fluoro-6-(4-(2-(isopropylamino)pyrimidin-4-yl)piperazin-1-yl)pyridin-3-yl)-2-oxooxazolidin-5-yl)methyl)acetamide (**6b**).

Compound **6b** was a pink solid; yield 44.4%.m. p. 196.8–199.5 °C.^{1}H NMR (600 MHz, DMSO-d_6) δ 8.24 (t, J = 6.0 Hz, 1H), 8.13 (d, J = 2.4 Hz, 1H), 7.93 (dd, J = 14.4, 2.4 Hz, 1H), 7.82 (d, J = 6.0 Hz, 1H), 6.31 (s, 1H), 6.04 (d, J = 6.0 Hz, 1H), 4.79 − 4.72 (m, 1H), 4.12 − 4.10 (m, 1H), 4.04 − 3.95 (m, 1H), 3.74 − 3.72 (m, 1H), 3.68 − 3.66 (m, 4H), 3.49 − 3.36 (m, 5H), 1.84 (s, 3H), 1.12 (d, J = 6.6 Hz, 6H), 1.08 − 0.94 (m, 1H). ^{13}C NMR (150 MHz, DMSO-d_6) δ 170.5, 162.7, 161.7, 157.2, 154.8, 149.1 (d, JC-F = 256.3 Hz), 146.0, 133.0, 129.9, 115.5, 115.4, 72.6, 47.8, 47.7, 47.6, 43.5, 42.2, 41.9, 23.1, 22.9. HRMS (ESI) (positive mode) m/z calculated for $C_{22}H_{29}FN_8O_3$: 472.53; Found: 473.189.

Raw data for the above products are presented in Supplementary Materials (Figures S4–S9).

3.2.3. General Procedure for the Synthesis of **6c–m**

To a solution of compound **5** (150 mg, 0.33 mmol) in dioxane (4 mL), p-toluene sulfonic acid monohydrate (11.4 mg, 0.066 mmol) and amine (1 mmol) were added and stirred at reflux overnight. After the reaction was complete, the filtrate was concentrated in vacuo. The mixture was extracted with DCM (5 mL × 3). The organic phase was washed with brine and concentrated in vacuo. The residue was purified by silica gel column chromatography (DCM/MeOH = 30:1) to yield compounds **6c–m.**

(S)-N-((3-(6-(4-(2-((2,2-difluoroethyl)amino)pyrimidin-4-yl)piperazin-1-yl)-5-fluoropyridin-3-yl)-2-oxooxazolidin-5-yl)methyl)acetamide (**6c**).

Compound **6c** was a pink solid; yield 66.7%.m. p. 228.1–231.2 °C.^{1}H NMR (600 MHz, DMSO-d_6) δ 8.24 (t, J = 6.0 Hz, 1H), 8.13 (d, J = 2.4 Hz, 1H), 7.94 (dd, J = 14.4, 2.4 Hz, 1H), 7.87 (d, J = 6.0 Hz, 1H), 7.02 (s, 1H), 6.20 (d, J = 6.0 Hz, 1H), 4.79 − 4.72 (m, 1H), 4.13 − 4.10 (m, 1H), 3.76 − 3.73 (m, 1H), 3.73 − 3.68 (m, 5H), 3.68 − 3.58 (m, 2H), 3.46 − 3.38 (m, 6H), 1.84 (s, 3H). ^{13}C NMR (150 MHz, DMSO-d_6) δ 170.5, 162.5, 154.8, 149.1 (d, JC-F = 257.2 Hz), 145.9, 145.8, 133.1, 133.0, 129.9, 115.6, 115.4, 72.6, 47.7, 47.64, 43.9, 43.7, 43.6, 41.9, 22.9. HRMS (ESI) (positive mode) m/z calculated for $C_{21}H_{25}F_3N_8O_3$: 494.48; Found: 495.163.

(S)-N-((3-(6-(4-(2-(allylamino)pyrimidin-4-yl)piperazin-1-yl)-5-fluoropyridin-3-yl)-2-oxooxazolidin-5-yl)methyl)acetamide (**6d**)

Compound **6d** was a white solid; yield 68.1%.m. p. 182.1–184.6 °C.^{1}H NMR (600 MHz, DMSO-d_6) δ 8.25 (t, J = 6.0 Hz, 1H), 8.14 (d, J = 2.4 Hz, 1H), 7.94 (dd, J = 14.4, 2.4 Hz, 1H), 7.85 (d, J = 6.6 Hz, 1H), 7.51 − 7.08 (m, 1H), 6.28 (d, J = 6.0 Hz, 1H), 5.92 − 5.86 (m, 1H), 5.19 (d, J = 17.4 Hz, 1H), 5.08 (d, J = 10.2 Hz, 1H), 4.77 − 4.73 (m, 1H), 4.13 − 4.10 (m, 1H), 3.93 − 3.91 (m, 2H), 3.78 − 3.75 (m, 4H), 3.74 − 3.72 (m, 1H), 3.43 − 3.39 (m, 6H), 1.84

(s, 3H). ^{13}C NMR (150 MHz, DMSO-d$_6$) δ 170.5, 162.0, 154.8, 149.1 (d, JC-F = 257.5 Hz), 145.8, 138.1, 136.4, 133.0, 130.0, 128.5, 126.0, 115.6, 115.4, 72.6, 47.6, 43.9, 43.4, 41.9, 22.9, 21.2. HRMS (ESI) (positive mode) *m/z* calculated for C$_{22}$H$_{27}$FN$_8$O$_3$: 470.51; Found: 471.133.

(S)-N-((3-(5-fluoro-6-(4-(2-(prop-2-yn-1-ylamino)pyrimidin-4-yl)piperazin-1-yl)pyridin-3-yl)-2-oxooxazolidin-5-yl)methyl)acetamide (**6e**)

Compound **6e** was a white solid; yield 44.9%. m. p. 185.6–188.7 °C.^{1}H NMR (600 MHz, DMSO-d$_6$) δ 8.29 (t, J = 6.0 Hz, 1H), 8.14 (d, J = 2.4 Hz, 1H), 7.94 (dd, J = 14.4, 2.4 Hz, 1H), 7.88 (d, J = 6.0 Hz, 1H), 7.22 (s, 1H), 6.23 (d, J = 6.0 Hz, 1H), 5.33 (s, 1H), 4.77 − 4.73 (m, 1H), 4.13 − 4.10 (m, 1H), 4.04 − 4.03 (m, 2H), 3.78 − 3.72 (m, 4H), 3.44 − 3.34 (m, 7H), 1.84 (s, 3H). ^{13}C NMR (150 MHz, DMSO-d$_6$) δ 170.5, 162.4, 154.8, 149.1 (d, JC-F = 256.9 Hz), 145.9, 145.8, 133.1, 133.0, 130.0, 115.6, 115.4, 72.6, 63.1, 52.5, 47.7, 43.7, 41.9, 30.6, 22.9, 7.7. HRMS (ESI) (positive mode) *m/z* calculated for C$_{22}$H$_{25}$FN$_8$O$_3$: 468.49; Found: 469.201.

(S)-N-((3-(5-fluoro-6-(4-(2-(4-methylpiperidin-1-yl)pyrimidin-4-yl)piperazin-1-yl)pyridin-3-yl)-2-oxooxazolidin-5-yl)methyl)acetamide (**6f**).

Compound **6f** was a pink solid; yield 64.4%. m. p. 198.1–200.5 °C.^{1}H NMR (600 MHz, DMSO-d$_6$) δ 8.24 (t, J = 6.0 Hz, 1H), 8.13 (d, J = 2.4 Hz, 1H), 7.93 (dd, J = 14.4, 2.4 Hz, 1H), 7.89 (d, J = 6.0 Hz, 1H), 6.08 (d, J = 6.0 Hz, 1H), 4.79 − 4.72 (m, 1H), 4.62 − 4.59 (m, 2H), 4.13 − 4.10 (m, 1H), 3.74 − 3.72 (m, 1H), 3.68 − 3.66 (m, 4H), 3.43 − 3.41 (m, 2H), 3.41 − 3.37 (m, 4H), 2.77 − 2.73 (m, 2H), 1.84 (s, 3H), 1.64 − 1.56 (m, 2H), 1.04 − 0.98 (m, 2H), 0.91 (d, J = 6.6 Hz, 3H). ^{13}C NMR (150 MHz, DMSO-d$_6$) δ 170.5, 162.7, 161.4, 157.1, 154.8, 149.1 (d, JC-F = 256.3 Hz), 146.0, 133.0, 129.9, 115.5, 115.4, 93.2, 72.6, 47.7, 44.0, 43.6, 41.9, 34.1, 31.3, 22.9, 22.4. HRMS (ESI) (positive mode) *m/z* calculated for C$_{25}$H$_{33}$FN$_8$O$_3$: 512.59; Found: 513.208.

(S)-N-((3-(5-fluoro-6-(4-(2-morpholinopyrimidin-4-yl)piperazin-1-yl)pyridin-3-yl)-2-oxooxazolidin-5-yl)methyl)acetamide (**6g**)

Compound **6g** was a white solid; yield 46.1%. m. p. 191.3–192.1 °C. ^{1}H NMR (600 MHz, DMSO-d$_6$) δ 8.24 (t, J = 6.0 Hz, 1H), 8.13 (d, J = 2.4 Hz, 1H), 7.96 − 7.90 (m, 2H), 6.17 (d, J = 6.0 Hz, 1H), 4.79 − 4.72 (m, 1H), 4.13 − 4.10 (m, 1H), 3.74 − 3.72 (m, 1H), 3.70 − 3.69 (m, 4H), 3.64 − 3.63 (m, 8H), 3.47 − 3.35 (m, 6H), 1.84 (s, 3H).^{13}C NMR (150 MHz, DMSO-d$_6$) δ 170.5, 162.6, 161.6, 157.1, 154.8, 150.0 (d, JC-F = 256.7 Hz), 146.0, 133.0, 129.9, 115.5, 115.4, 94.1, 72.6, 66.6, 47.7, 44.4, 43.6, 41.9, 22.9. HRMS (ESI) (positive mode) m/z calculated for C$_{23}$H$_{29}$FN$_8$O$_4$: 500.54; Found: 501.176.

(S)-N-((3-(5-fluoro-6-(4-(2-((3-morpholinopropyl)amino)pyrimidin-4-yl)piperazin-1-yl)pyridin-3-yl)-2-oxooxazolidin-5-yl)methyl)acetamide (**6h**)

Compound **6h** was brown oil; yield 48.7%. ^{1}H NMR (600 MHz, DMSO-d$_6$) δ 8.28 (t, J = 6.0 Hz, 1H), 8.12 (d, J = 2.4 Hz, 1H), 7.92 (dd, J = 14.4, 2.4 Hz, 1H), 7.81 (d, J = 6.0 Hz, 1H), 6.57 (s, 1H), 6.03 (d, J = 6.0 Hz, 1H), 4.77 − 4.73 (m, 1H), 4.12 − 4.09 (m, 1H), 3.75 − 3.73 (m, 1H), 3.67 − 3.65 (m, 4H), 3.57 − 3.56 (m, 4H), 3.44 − 3.42 (m, 4H), 3.38 − 3.35 (m, 4H), 3.27 − 3.23 (m, 2H), 2.33 − 2.30 (m, 4H), 1.85 (s, 3H), 1.66 − 1.64 (m, 2H). ^{13}C NMR (150 MHz, DMSO-d$_6$) δ 170.6, 162.7, 162.3, 157.2, 154.8, 149.1 (d, JC-F = 257.1 Hz), 145.9, 132.9, 129.8, 115.5, 115.3, 72.6, 66.7, 56.7, 53.8, 47.7, 46.1, 43.5, 41.9, 26.5, 22.9, 7.6. HRMS (ESI) (positive mode) *m/z* calculated for C$_{26}$H$_{35}$FN$_8$O$_4$: 557.63; Found: 558.256.

(S)-N-((3-(5-fluoro-6-(4-(2-(phenylamino)pyrimidin-4-yl)piperazin-1-yl)pyridin-3-yl)-2-oxooxazolidin-5-yl)methyl)acetamide (**6i**)

Compound **6i** was a white solid; yield 43%. m. p. 190.6–194.4 °C.^{1}H NMR (600 MHz, DMSO-d$_6$) δ 9.17 (s, 1H), 8.24 (t, J = 6.0 Hz, 1H), 8.14 (d, J = 2.4 Hz, 1H), 8.00 (d, J = 6.0 Hz, 1H), 7.95 (dd, J = 14.4, 2.4 Hz, 1H), 7.73 − 7.68 (m, 2H), 7.30 − 7.24 (m, 2H), 6.92 (t, J = 7.2 Hz, 1H), 6.36 (d, J = 6.0 Hz, 1H), 4.79 − 4.72 (m, 1H), 4.14 − 4.11 (m, 1H), 3.79 − 3.77 (m, 4H), 3.75 − 3.72 (m, 1H), 3.48 − 3.39 (m, 6H), 1.84 (s, 3H). ^{13}C NMR (150 MHz, DMSO-d$_6$) δ 170.5, 165.2, 162.5, 154.8, 149.1 (d, JC-F = 256.2 Hz), 145.7, 141.2, 140.8, 133.0, 129.8, 128.9, 121.8, 119.4, 117.3, 115.6, 95.8, 72.6, 47.7, 43.8, 41.9, 22.9. HRMS (ESI) (positive mode) *m/z* calculated for C$_{25}$H$_{27}$FN$_8$O$_3$: 506.54; Found: 507.161.

(S)-N-((3-(6-(4-(2-(benzylamino)pyrimidin-4-yl)piperazin-1-yl)-5-fluoropyridin-3-yl)-2-oxooxazolidin-5-yl)methyl)acetamide (**6j**)

Compound **6j** was a white solid; yield 41.5%. m. p. 202.7–204.6 °C.^{1}H NMR (600 MHz, DMSO-d$_6$) δ 8.24 (t, J = 6.0 Hz, 1H), 8.13 (d, J = 2.4 Hz, 1H), 7.93 (dd, J = 14.4, 2.4 Hz, 1H), 7.82 (d, J = 6.0 Hz, 1H), 7.32 − 7.24 (m, 5H), 7.22 − 7.16 (m, 1H), 6.07 (d, J = 6.0 Hz, 1H), 4.79 − 4.72 (m, 1H), 4.14 − 4.10 (m, 1H), 3.74 − 3.72 (m, 1H), 3.74 − 3.64 (m, 4H), 3.47 − 3.38 (m, 2H), 3.36 − 3.34 (m, 4H), 1.84 (s, 3H). ^{13}C NMR (150 MHz, DMSO-d$_6$) δ 170.5, 162.6, 162.3, 154.8, 150.0 (d, JC-F = 256.7 Hz), 146.0, 145.9, 141.7, 133.0, 129.8, 128.5, 127.6, 126.8, 115.5, 115.4, 72.6, 47.8, 44.5, 43.5, 41.9, 22.9. HRMS (ESI) (positive mode) m/z calculated for C$_{26}$H$_{29}$FN$_8$O$_3$: 520.57; Found: 521.185.

(S)-N-((3-(5-fluoro-6-(4-(2-(naphthalen-1-ylamino)pyrimidin-4-yl)piperazin-1-yl)pyridin-3-yl)-2-oxooxazolidin-5-yl)methyl)acetamide (**6k**)

Compound **6k** was a brown solid; yield 59.3%. m. p. 221.8–223.1 °C.^{1}H NMR (600 MHz, DMSO-d6) δ 8.95 (s, 1H), 8.24 (t, J = 6.0 Hz, 1H), 8.14–8.07 (m, 2H), 7.95 − 7.88 (m, 3H), 7.79 (d, J = 7.2 Hz, 1H), 7.67 (d, J = 8.2 Hz, 1H), 7.51–7.44 (m, 3H), 6.29 (d, J = 6.0 Hz, 1H), 4.77–4.72 (m, 1H), 4.15–4.06 (m, 1H), 3.76–3.70 (m, 1H), 3.69–3.64 (m, 4H), 3.43–3.40 (m, 2H), 3.39–3.36(m, 4H), 1.84 (s, 3H). ^{13}C NMR (150 MHz, DMSO-d$_6$) δ 170.6, 162.1, 154.8, 152.4, 149.1 (d, JC-F = 257.1 Hz), 146.0, 145.7, 134.9, 134.4, 133.0, 130.0, 128.7, 128.6, 126.4, 126.1, 126.0, 125.1, 123.4, 121.7, 115.6, 115.4, 95.8, 72.6, 63.1, 52.5, 22.9, 7.7. HRMS (ESI) (positive mode) m/z calculated for C$_{29}$H$_{29}$FN$_8$O$_3$: 556.60; Found: 557.197.

(S)-N-((3-(5-fluoro-6-(4-(2-(quinolin-5-ylamino)pyrimidin-4-yl)piperazin-1-yl)pyridin-3-yl)-2-oxooxazolidin-5-yl)methyl)acetamide (**6l**)

Compound **6l** was a white solid; yield 43%. m. p. 226.2–232.2 °C.^{1}H NMR (600 MHz, DMSO-d$_6$) δ 9.15 (s, 1H), 8.87 (dd, J = 4.2, 1.8 Hz, 1H), 8.53 − 8.48 (m, 1H), 8.24 (t, J = 6.0 Hz, 1H), 8.15 − 8.12 (m, 1H), 7.99 − 7.90 (m, 2H), 7.87 (dd, J = 7.2, 1.2 Hz, 1H), 7.77 − 7.71 (m, 2H), 7.489 − 7.47 (m, 1H), 6.33 (d, J = 6.0 Hz, 1H), 4.79 − 4.72 (m, 1H), 4.13 − 4.10 (m, 1H), 3.74 − 3.72 (m, 1H), 3.68 − 3.66 (m, 4H), 3.43 − 3.41 (m, 2H), 3.39 − 3.37 (m, 4H), 1.84 (s, 3H). ^{13}C NMR (150 MHz, DMSO-d$_6$) δ 170.5, 162.5, 161.1, 157.3, 154.8, 149.7 (d, JC-F = 259.1 Hz), 148.3, 145.9, 136.9, 133.0, 132.6, 129.9, 129.6, 124.7, 123.6, 120.7, 120.6, 115.6, 115.4, 107.8, 95.9, 72.6, 47.7, 43.5, 41.9, 22.9. HRMS (ESI) (positive mode) m/z calculated for C$_{28}$H$_{28}$FN$_9$O$_3$: 557.59; Found: 558.207.

(S)-N-((3-(6-(4-(2-((6-chloropyridin-3-yl)amino)pyrimidin-4-yl)piperazin-1-yl)-5-fluoropyridin-3-yl)-2-oxooxazolidin-5-yl)methyl)acetamide (**6m**)

Compound **6m** was a white solid; yield 45.8%. m. p. 134.4–135.6 °C.^{1}H NMR (600 MHz, DMSO-d$_6$) δ 9.46 (s, 1H), 8.74 (d, J = 3.0 Hz, 1H), 8.27 − 8.19 (m, 2H), 8.14 (d, J = 2.4 Hz, 1H), 8.05 (d, J = 6.0 Hz, 1H), 7.94 (dd, J = 14.4, 2.4 Hz, 1H), 7.40 (d, J = 9.0 Hz, 1H), 6.40 (d, J = 6.0 Hz, 1H), 4.79 − 4.72 (m, 1H), 4.14 − 4.11 (m, 1H), 3.78 − 3.71 (m, 5H), 3.47 − 3.42 (m, 6H), 1.84 (s, 3H). ^{13}C NMR (150 MHz, DMSO-d$_6$) δ 170.5, 162.5, 159.5, 157.1, 154.8, 149.1 (d, JC-F = 256.5 Hz), 145.8, 141.3, 140.2, 137.9, 133.0, 129.9, 129.2, 124.2, 115.6, 115.4, 96.6, 72.6, 47.6, 43.7, 41.9, 22.9. HRMS (ESI) (positive mode) m/z calculated for C$_{24}$H$_{25}$ClFN$_9$O$_3$: 541.97; Found: 542.132.

Raw data for the above products are presented in Supplementary Materials (Figures S10–S42).

3.2.4. General Procedure for the Synthesis of **7a** and **7c-n**

A solution of compound **4** (130 mg, 0.3 mmol) in DCM (5 mL) at 0 °C was dropwise added to TFA (1 mL) and then stirred for 2 h. After the reaction was complete, TEA was added to the solution at 0 °C to adjust pH. The filtrate was concentrated in vacuo. To a solution of the concentrate in ethanol (3 mL) was added TEA (83 μL, 1 mmol) and pyrimidine derivative (0.4 mmol), and then stirred at reflux overnight. After the reaction was complete and concentrated, the mixture was extracted with DCM (5 mL × 3). The organic phase was washed with brine and concentrated in vacuo. The residue was purified by silica gel column chromatography (DCM/MeOH = 30:1) to yield compounds **7a** and **7c-n**.

(S)-N-((3-(6-(4-(6-chloropyrimidin-4-yl)piperazin-1-yl)-5-fluoropyridin-3-yl)-2-oxooxazolidin-5-yl)methyl)acetamide (**7a**)

Compound **7a** was a white solid; yield 45.1%. m. p. 190.0–191.1 °C.^{1}H NMR (600 MHz, DMSO-d$_6$) δ 8.37 (s, 1H), 8.24 (t, J = 6.0 Hz, 1H), 8.14 (d, J = 2.4 Hz, 1H), 7.94 (dd, J = 14.4,

2.4 Hz, 1H), 7.02 (s, 1H), 4.79 − 4.72 (m, 1H), 4.14 − 4.10 (m, 1H), 3.81 − 3.75 (m, 4H), 3.74 − 3.71 (m, 1H), 3.43 − 3.42 (m, 6H), 1.84 (s, 3H). ^{13}C NMR (150 MHz, DMSO-d_6) δ 170.5, 162.7, 159.7, 158.5, 154.8, 148.2 (d, JC-F = 256.7 Hz), 145.6, 133.0, 129.99, 115.6, 102.3, 72.6, 47.6, 47.5, 43.8, 41.9, 22.9. HRMS (ESI) (positive mode) *m/z* calculated for $C_{19}H_{21}ClFN_7O_3$: 449.87; Found: 450.106.

(S)-N-((3-(5-fluoro-6-(4-(5-methylpyrimidin-2-yl)piperazin-1-yl)pyridin-3-yl)-2-oxooxazolidin-5-yl)methyl)acetamide (**7c**)

Compound **7c** was a white solid; yield 49.4%. m. p. 195.1–197.3 °C. ^{1}H NMR (600 MHz, DMSO-d_6) δ 8.26 − 8.23 (m, 3H), 8.13 (d, J = 2.4 Hz, 1H), 7.93 (dd, J = 14.4, 2.4 Hz, 1H), 4.77 − 4.73 (m, 1H), 4.13 − 4.10 (m, 1H), 3.85 − 3.80 (m, 4H), 3.76 − 3.70 (m, 1H), 3.43 − 3.37 (m, 6H), 2.10 (s, 3H), 1.84 (s, 3H). ^{13}C NMR (150 MHz, DMSO-d_6) δ 160.7, 158.2, 154.8, 149.2 (d, JC-F = 255.3 Hz), 146.1, 133.0, 130.0, 119.1, 115.5, 115.4, 72.6, 47.9, 46.2, 43.9, 22.9, 14.1, 9.1. HRMS (ESI) (positive mode) *m/z* calculated for $C_{20}H_{24}FN_7O_3$: 429.46; Found: 430.181.

(S)-N-((3-(6-(4-(5-bromopyrimidin-2-yl)piperazin-1-yl)-5-fluoropyridin-3-yl)-2-oxooxazolidin-5-yl)methyl)acetamide (**7d**)

Compound **7d** was a white solid; yield 47.6%. m. p. 196.1–196.3 °C. ^{1}H NMR (600 MHz, DMSO-d_6) δ 8.50 (s, 2H), 8.24 (t, J = 6.0 Hz, 1H), 8.13 (d, J = 2.4 Hz, 1H), 7.94 (dd, J = 14.4, 2.4 Hz, 1H), 4.77 − 4.73 (m, 1H), 4.14 − 4.10 (m, 1H), 3.88 − 3.83 (m, 4H), 3.74 − 3.71 (m, 1H), 3.43 − 3.33 (m, 6H), 1.84 (s, 3H). ^{13}C NMR (150 MHz, DMSO-d_6) δ 170.5, 166.3, 160.0, 158.5, 154.8, 150.8 (d, JC-F = 253.7 Hz), 133.0, 129.9, 115.3, 106.1, 72.6, 47.6, 43.8, 41.9, 39.0, 22.9. HRMS (ESI) (positive mode) *m/z* calculated for $C_{19}H_{21}BrFN_7O_3$: 494.33; Found: 496.095.

(S)-N-((3-(6-(4-(2-aminopyrimidin-4-yl)piperazin-1-yl)-5-fluoropyridin-3-yl)-2-oxooxazolidin-5-yl)methyl)acetamide (**7e**)

Compound **7e** was a white solid; yield 60.9%. m. p. 195.6–196.7 °C. ^{1}H NMR (600 MHz, DMSO-d_6) δ 8.28 − 8.25 (m, 1H), 8.15 (d, J = 2.4 Hz, 1H), 7.97 − 7.88 (m, 3H), 7.89 (dd, J = 7.8, 2.4 Hz, 1H), 6.57 (d, J = 7.8 Hz, 1H), 4.78 − 4.74 (m, 1H), 4.14 − 4.11 (m, 1H), 3.75 − 3.72 (m, 1H), 3.47 − 3.46 (m, 4H), 3.43 − 3.41 (m, 4H), 1.84 (s, 3H). ^{13}C NMR (150 MHz, DMSO-d_6) δ 170.5, 161.7, 155.1, 154.8, 149.1 (d, JC-F = 256.4 Hz), 145.4, 143.4, 133.0, 130.1, 115.6, 115.5, 95.4, 72.7, 47.6, 47.5, 41.9, 22.9. HRMS (ESI) (positive mode) *m/z* calculated for $C_{19}H_{23}FN_8O_3$: 430.44; Found: 431.144.

(S)-N-((3-(6-(4-(4-aminopyrimidin-2-yl)piperazin-1-yl)-5-fluoropyridin-3-yl)-2-oxooxazolidin-5-yl)methyl)acetamide (**7f**)

Compound **7f** was a white solid; yield 60.9%. m. p. 196.6–197.7 °C. ^{1}H NMR (600 MHz, DMSO-d_6) δ 8.25 (t, J = 6.0 Hz, 1H), 8.14 (d, J = 2.4 Hz, 1H), 7.94 (dd, J = 14.4, 2.4 Hz, 1H), 7.77 (d, J = 6.0 Hz, 1H), 7.48 − 7.10 (m, 2H), 5.94 (d, J = 6.0 Hz, 1H), 4.79 − 4.72 (m, 1H), 4.13 − 4.10 (m, 1H), 3.80 − 3.78 (m, 4H), 3.75 − 3.72 (m, 1H), 3.43 − 3.40 (m, 6H), 1.84 (s, 3H). ^{13}C NMR (150 MHz, DMSO-d_6) δ 170.5, 164.5, 154.8, 149.1 (d, JC-F = 256.7 Hz), 145.9, 138.1, 133.0, 130.0, 128.5, 126.0, 115.6, 72.6, 47.7, 43.9, 41.9, 22.9, 21.3. HRMS (ESI) (positive mode) *m/z* calculated for $C_{19}H_{23}FN_8O_3$: 430.44; Found: 431.141.

(S)-N-((3-(6-(4-(4,6-dichloropyrimidin-2-yl)piperazin-1-yl)-5-fluoropyridin-3-yl)-2-oxooxazolidin-5-yl)methyl)acetamide(**7g**)*and (S)-N-((3-(6-(4-(2,6-dichloropyrimidin-4-yl)piperazin-1-yl)-5-fluoropyridin-3-yl)-2-oxooxazolidin-5-yl)methyl)acetamide* (**7h**)

Compounds **7g** and **7h** were both white solids, yields were 13.8% and 44.7% respectively, m. p. 191.3–192.5 °C and m. p. 195.2–197.1 °C respectively.

Compound **7g**, ^{1}H NMR (600 MHz, DMSO-d_6) δ 8.24 (t, J = 6.0 Hz, 1H), 8.14 (d, J = 2.4 Hz, 1H), z7.94 (dd, J = 14.4, 2.4 Hz, 1H), 6.98 (s, 1H), 4.77 − 4.73 (m, 1H), 4.14 − 4.10 (m, 1H), 3.88 − 3.84 (m, 4H), 3.75 − 3.72 (m, 1H), 3.44 − 3.41 (m, 6H), 1.84 (s, 3H). ^{13}C NMR (150 MHz, DMSO-d_6) δ 170.5, 161.6, 160.5, 154.8, 148.2 (d, J = 256.7 Hz), 145.7, 132.9, 130.0, 115.4, 108.2, 72.6, 47.6, 47.5, 43.9, 41.9, 22.9. HRMS (ESI) (positive mode) *m/z* calculated for $C_{19}H_{20}Cl_2FN_7O_3$: 483.10; Found: 484.103.

Compound **7h**, ^{1}H NMR (600 MHz, DMSO-d_6) δ 8.24 (t, J = 6.0 Hz, 1H), 8.14 (d, J = 2.4 Hz, 1H), 7.94 (dd, J = 14.4, 2.4 Hz, 1H), 7.08 (s, 1H), 4.77 − 4.74 (m, 1H), 4.13 − 4.10 (m, 1H), 3.87 − 3.71 (m, 5H), 3.44 − 3.42 (m, 6H), 1.84 (s, 3H). ^{13}C NMR (150 MHz, DMSO-d_6) δ 170.5, 163.4, 159.6, 159.0, 154.8, 149.1 (d, JC-F = 257.1 Hz), 145.5, 133.0, 130.0,

115.4, 101.4, 72.6, 47.6, 47.4, 43.7, 41.9, 22.9. HRMS (ESI) (positive mode) *m/z* calculated for $C_{19}H_{20}Cl_2FN_7O_3$: 483.10; Found: 484.104.

*(S)-N-((3-(6-(4-(2-chloro-5-fluoropyrimidin-4-yl)piperazin-1-yl)-5-fluoropyridin-3-yl)-2-oxoo-xazolidin-5-yl)methyl)acetamide (**7i**)*

Compound **7i** was a white solid; yield 70.1%. m. p. 204.4–205.5 °C.^{1}H NMR (600 MHz, DMSO-d$_6$) δ 8.25 − 8.21 (m, 2H), 8.14 (d, J = 2.4 Hz, 1H), 7.94 (dd, J = 14.4, 2.4 Hz, 1H), 4.79 − 4.72 (m, 1H), 4.14 − 4.10 (m, 1H), 3.90 − 3.86 (m, 4H), 3.75 − 3.71 (m, 1H), 3.48 − 3.46 (m, 4H), 3.43 − 3.41 (m, 2H), 1.84 (s, 3H). ^{13}C NMR (150 MHz, DMSO-d$_6$) δ 170.5, 154.8, 153.5, 152.5, 149.1 (d, JC-F = 257.0 Hz), 147.1 (d, JC-F = 256.4 Hz), 145.6, 144.7, 133.0, 130.0, 115.6, 72.6, 47.6, 45.8, 41.9, 40.5, 22.9. HRMS (ESI) (positive mode) *m/z* calculated for $C_{19}H_{20}ClF_2N_7O_3$: 467.86; Found: 468.113.

*(S)-N-((3-(6-(4-(2,5-dichloropyrimidin-4-yl)piperazin-1-yl)-5-fluoropyridin-3-yl)-2-oxooxazo-lidin-5-yl)methyl)acetamide (**7j**)*

Compound **7j** was a white solid; yield 48.6%. m. p. 193.5–194.2 °C.^{1}H NMR (600 MHz, DMSO-d$_6$) δ 8.35 (s, 1H), 8.24 (t, J = 6.0 Hz, 1H), 8.14 (d, J = 2.4 Hz, 1H), 7.94 (dd, J = 14.4, 2.4 Hz, 1H), 4.77 − 4.73 (m, 1H), 4.14 − 4.10 (m, 1H), 3.91 − 3.86 (m, 4H), 3.75 − 3.72 (m, 1H), 3.51 − 3.46 (m, 4H), 3.43 − 3.41 (m, 2H), 1.84 (s, 3H). ^{13}C NMR (150 MHz, DMSO-d$_6$) δ 170.5, 160.4, 159.1, 157.1, 154.8, 148.3 (d, JC-F = 256.7 Hz), 133.0, 130.0, 115.5, 115.1, 72.6, 47.6, 47.6, 47.0, 41.9, 22.9. HRMS (ESI) (positive mode) *m/z* calculated for $C_{19}H_{20}Cl_2FN_7O_3$: 483.10; Found: 484.099.

*(S)-N-((3-(6-(4-(5-bromo-2-chloropyrimidin-4-yl)piperazin-1-yl)-5-fluoropyridin-3-yl)-2-oxoo-xazolidin-5-yl)methyl)acetamide (**7k**)*

Compound **7k** was a white solid. m. p. 196.7–197.6 °C. ^{1}H NMR (600 MHz, DMSO-d$_6$) δ 8.46 (s, 1H), 8.24 (t, J = 6.0 Hz, 1H), 8.14 (d, J = 2.4 Hz, 1H), 7.94 (dd, J = 14.4, 2.4 Hz, 1H), 4.77 − 4.73 (m, 1H), 4.14 − 4.10 (m, 1H), 3.87 − 3.83 (m, 4H), 3.75 − 3.72 (m, 1H), 3.50 − 3.46 (m, 4H), 3.43 − 3.41 (m, 2H), 1.84 (s, 3H). ^{13}C NMR (150 MHz, DMSO-d$_6$) δ 170.5, 162.7, 161.8, 157.8, 154.8, 149.1 (d, JC-F = 257.1 Hz), 145.6, 133.0, 130.0, 115.5, 104.1, 72.6, 47.6, 47.6, 47.3, 41.9, 22.9. HRMS (ESI) (positive mode) *m/z* calculated for $C_{19}H_{20}BrClFN_7O_3$: 528.77; Found: 530.054.

*(S)-N-((3-(6-(4-(2-chloro-5-methylpyrimidin-4-yl)piperazin-1-yl)-5-fluoropyridin-3-yl)-2-oxoo-xazolidin-5-yl)methyl)acetamide (**7l**)*

Compound **7l** was a white solid; yield 58.9%. m. p. 198.8–200.8 °C. ^{1}H NMR (600 MHz, DMSO-d$_6$) δ 8.24 (t, J = 6.0 Hz, 1H), 8.14 (d, J = 2.4 Hz, 1H), 8.06 (s, 1H), 7.93 (dd, J = 14.4, 2.4 Hz, 1H), 4.79 − 4.72 (m, 1H), 4.14 − 4.10 (m, 1H), 3.74 − 3.72 (m, 1H), 3.70 − 3.65 (m, 4H), 3.48 − 3.44 (m, 4H), 3.43 − 3.41 (m, 2H), 2.24 (s, 3H), 1.84 (s, 3H). ^{13}C NMR (150 MHz, DMSO-d$_6$) δ 170.5, 165.0, 160.0, 157.2, 154.8, 149.1 (d, JC-F = 257.1 Hz), 145.8, 133.0, 130.0, 116.2, 115.4, 72.6, 47.8, 47.6, 46.9, 41.9, 22.9, 17.3. HRMS (ESI) (positive mode) *m/z* calculated for $C_{20}H_{23}ClFN_7O_3$: 463.90; Found: 464.117.

*Ethyl(S)-4-(4-(5-(5-(acetamidomethyl)-2-oxooxazolidin-3-yl)-3-fluoropyridin-2-yl)piperazin-1-yl)-2-(methylthio)pyrimidine-5-carboxylate (**7m**)*

Compound **7m** was a white solid; yield 50.6%. m. p. 210.1–213.1 °C. ^{1}H NMR (600 MHz, DMSO-d$_6$) δ 8.45 (s, 1H), 8.26 (t, J = 6.0 Hz, 1H), 8.11 (d, J = 2.4 Hz, 1H), 7.92 (dd, J = 14.4, 2.4 Hz, 1H), 4.79 − 4.72 (m, 1H), 4.36 − 4.17 (m, 2H), 4.14 − 4.09 (m, 1H), 3.76 − 3.72 (m, 1H), 3.68 − 3.66 (m, 4H), 3.46 − 3.44 (m, 4H), 3.43 − 3.41 (m, 2H), 2.48 (s, 3H), 1.85 (s, 3H), 1.37 − 1.25 (m, 3H). ^{13}C NMR (150 MHz, DMSO-d$_6$) δ 172.6, 170.5, 165.9, 159.8, 159.3, 154.8, 149.0 (d, JC-F = 257.0 Hz), 145.6, 132.9, 129.8, 115.3, 105.7, 72.6, 61.4, 47.6, 47.5, 47.3, 41.9, 22.9, 14.5, 14.1. HRMS (ESI) (positive mode) *m/z* calculated for $C_{23}H_{28}FN_7O_5S$: 533.58; Found: 534.132.

*(S)-N-((3-(5-fluoro-6-(4-(2,5,6-trichloropyrimidin-4-yl)piperazin-1-yl)pyridin-3-yl)-2-oxooxa-zolidin-5-yl)methyl)acetamide (**7n**)*

Compound **7n** was a white solid; yield 71.4%. m. p. 210.0–211.1 °C. ^{1}H NMR (600 MHz, DMSO-d$_6$) δ 8.24 (t, J = 6.0 Hz, 1H), 8.14 (d, J = 2.4 Hz, 1H), 7.94 (dd, J = 14.4, 2.4 Hz, 1H), 4.79 − 4.72 (m, 1H), 4.13 − 4.10 (m, 1H), 3.92 − 3.81 (m, 4H), 3.75 − 3.72 (m, 1H), 3.52 − 3.47 (m, 4H), 3.44 − 3.39 (m, 2H), 1.84 (s, 3H). ^{13}C NMR (150 MHz, DMSO-d$_6$) δ 170.5,

161.9, 159.0, 155.1, 154.8, 149.1 (d, JC-F = 255.8 Hz), 145.6, 133.0, 129.8, 115.4, 112.4, 72.6, 47.8, 47.6, 47.5, 41.9, 22.9. HRMS (ESI) (positive mode) *m/z* calculated for $C_{19}H_{19}Cl_3FN_7O_3$: 518.76; Found: 520.066.

Raw data for the above products are presented in Supplementary Materials (Figures S43, S45 and S49–S84).

3.3. MIC Determination

The antibacterial activity of the synthesized derivatives was determined by the broth dilution method [42]. The strains, including *Staphylococcus aureus* (ATCC25923), *Streptococcus pneumoniae* (ATCC49619), *Enterococcus faecalis* (ATCC29212), *Bacillus subtilis* (ATCC6633), *Escherichia coli* (ATCC25922), *Listeria monocytogenes* (ATCC19111), *Staphylococcus xylosus (ATCC35924)*, methicillin-resistant *Staphylococcus aureus*, vancomycin-resistant *Enterococcus faecalis*, linezolid-resistant *Staphylococcus aureus,* and linezolid-resistant *Streptococcus pneumoniae*, were incubated in Mueller-Hinton (MH) medium at 37 °C to mid-logarithm (OD_{600} = 0.5). The bacteria were diluted to 10^5 CFU/ mL and added to the 96-well plate, followed by a series of diluted synthesized derivatives (from 128 to 0.25 μg/mL). After incubation at 37 °C for 16–18 h, the minimum inhibitory concentration (MIC) value was the minimum drug concentration without bacterial growth.

3.4. Molecular Docking Studies

The 3D structure of the 50S ribosomal subunit (PDB code: 3CPW) [43] was obtained from the Protein Data Bank and processed by PyMOL 2.5. The original ligand and protein were deleted, and only the required RNA chains were retained and imported into the Auto-Dock for use. The ligand was drawn with ChemOffice2010 Version and imported into the Auto-Dock for later use. The Auto-Dock 4.2.6® software was used for the molecular docking process, and the obtained results were imported into PyMOL 2.5 software in the form of complexes for visual analysis.

3.5. Inhibition of Biofilm Formation Assay

Anti-biofilm activity inhibits biofilm formation and was measured by the crystal violet method [44]. The strains to be tested were placed in a test tube containing 5 mL Tryptic Soy Broth (TSB) and incubated at 37 °C for 24 h. Then the suspension was diluted to 10^6 CFU/mL and added to a sterile 96-well culture plate, filled with 100 μL per well. All compounds were added to the well according to the selected concentration gradient and incubated at 37 °C for 24 h. After the biofilm was grown, the culture medium was removed from each well, washed twice with sterile PBS, fixed with methanol, and stained with 150 μL 0.1% crystal violet solution at room temperature. Remove the excess solution, wash it twice with water, and add 125 μL 33% acetic acid to each dyeing well for 5 min to dissolve the dye. The microplate reader was used to read at 600 nm to assess the minimum concentration of biofilm inhibition.

3.6. Cytotoxicity Assay

The MTT method was used to detect the effect of typical derivatives on Hela cell viability [45]. Cells (5×10^4 cells/well) were added to a 96-well plate for 24 h in humidified 5% (V/V) CO_2/ air at 37 °C. A series of liquid medicines (8, 16, 32, 64, 128, 256, 500, and 1000 μg/mL) were added and incubated for 48 h. Cells treated with equal volumes of DMSO were used as controls. Add 10 μL MTT solution (0.5%) to each well and incubate for 4 h at 37 °C under dark conditions. The culture medium in all wells was discarded. Then 100 μL DMSO was quickly added to each wall and shaken at low speed to dissolve the formed crystals. The absorbance was measured at 570 nm. The cell viability was calculated as follows: cell viability (%) = (treatment sample OD_{570} − empty OD_{570})/(control OD_{570} − empty OD_{570}).

4. Conclusions

In summary, a library of 28 novel 3-(5-fluoropyridine-3-yl)-2-oxazolidinone derivatives was designed, synthesized, and evaluated for their antibacterial properties. The results show that most of the synthesized compounds have potential antibacterial activity against gram-positive bacteria. Amongst them, compounds **7i-l** exhibited a better antibacterial effect. The molecular docking results of compounds **7j** and PTC were studied to predict the mechanism of action. Further results demonstrated that these compounds have excellent ability to inhibit biofilm formation and meager cytotoxicity. These results provide a basis and reference for the discovery of novel antibacterial compounds and the development of new drugs.

Supplementary Materials: The following are available online at https://www.mdpi.com/article/10.3390/molecules28114267/s1. Figure S1: ^{1}H NMR Spectrum of **5**; Figure S2: ^{13}C NMR Spectrum of **5**; Figure S3: ES-MS for compound **5**; Figure S4: ^{1}H NMR Spectrum of **6a**; Figure S5: ^{13}C NMR Spectrum of **6a**; Figure S6: ES-MS for compound **6a**; Figure S7: ^{1}H NMR Spectrum of **6b**; Figure S8: ^{13}C NMR Spectrum of **6b**; Figure S9: ES-MS for compound **6b**; Figure S10: ^{1}H NMR Spectrum of 6c; Figure S11: ^{13}C NMR Spectrum of **6c**; Figure S12: ES-MS for compound **6c**; Figure S13: ^{1}H NMR Spectrum of **6d**; Figure S14: ^{13}C NMR Spectrum of **6d**; Figure S15: ES-MS for compound **6d**; Figure S16: ^{1}H NMR Spectrum of **6e**; Figure S17: ^{13}C NMR Spectrum of **6e**; Figure S18: ES-MS for compound **6e**; Figure S19 ^{1}H NMR Spectrum of **6f**; Figure S20: ^{13}C NMR Spectrum of **6f**; Figure S21: ES-MS for compound **6f**; Figure S22: ^{1}H NMR Spectrum of **6g**; Figure S23: ^{13}C NMR Spectrum of **6g**; Figure S24: ES-MS for compound **6g**; Figure S25: ^{1}H NMR Spectrum of **6h**; Figure S26: ^{13}C NMR Spectrum of **6h**; Figure S27: ES-MS for compound **6h**; Figure S28: ^{1}H NMR Spectrum of **6i**; Figure S29: ^{13}C NMR Spectrum of **6i**; Figure S30: ES-MS for compound **6i**; Figure S31: ^{1}H NMR Spectrum of **6j**; Figure S32: ^{13}C NMR Spectrum of **6j**; Figure S33: ES-MS for compound **6j**; Figure S34: ^{1}H NMR Spectrum of **6k**; Figure S35: ^{13}C NMR Spectrum of **6k**; Figure S36: ES-MS for compound **6k**; Figure S37: ^{1}H NMR Spectrum of **6l**; Figure S38: ^{13}C NMR Spectrum of **6l**; Figure S39: ES-MS for compound **6l**; Figure S40: ^{1}H NMR Spectrum of **6m**; Figure S41: ^{13}C NMR Spectrum of **6m**; Figure S42: ES-MS for compound **6m**; Figure S43: ^{1}H NMR Spectrum of **7a**; Figure S44: ^{13}C NMR Spectrum of **7a**; Figure S45: ES-MS for compound **7a**; Figure S46: ^{1}H NMR Spectrum of **7b**; Figure S47: ^{13}C NMR Spectrum of **7b**; Figure S48: ES-MS for compound **7b**; Figure S49: ^{1}H NMR Spectrum of **7c**; Figure S50: ^{13}C NMR Spectrum of **7c**; Figure S51: ES-MS for compound **7c;** Figure S52: ^{1}H NMR Spectrum of **7d**; Figure S53: ^{13}C NMR Spectrum of **7d**; Figure S54: ES-MS for compound **7d**; Figure S55: ^{1}H NMR Spectrum of **7e**; Figure S56: ^{13}C NMR Spectrum of **7e**; Figure S57: ES-MS for compound **7e**; Figure S58: ^{1}H NMR Spectrum of **7f**; Figure S59: ^{13}C NMR Spectrum of **7f**; Figure S60: ES-MS for compound **7f**; Figure S61: ^{1}H NMR Spectrum of **7g**; Figure S62: ^{13}C NMR Spectrum of **7g**; Figure S63: ES-MS for compound **7g**; Figure S64: ^{1}H NMR Spectrum of **7h**; Figure S65: ^{13}C NMR Spectrum of **7h**; Figure S66: ES-MS for compound **7h**; Figure S67: ^{1}H NMR Spectrum of **7i**; Figure S68: ^{13}C NMR Spectrum of **7i**; Figure S69: ES-MS for compound **7i**; Figure S70: ^{1}H NMR Spectrum of **7j**; Figure S71: ^{13}C NMR Spectrum of **7j**; Figure S72: ES-MS for compound **7j**; Figure S73: ^{1}H NMR Spectrum of **7k**; Figure S74: ^{13}C NMR Spectrum of **7k**; Figure S75: ES-MS for compound **7k**; Figure S76: ^{1}H NMR Spectrum of **7l**; Figure S77: ^{13}C NMR Spectrum of **7l**; Figure S78: ES-MS for compound **7l**; Figure S79: ^{1}H NMR Spectrum of **7m**; Figure S80: ^{13}C NMR Spectrum of **7m**; Figure S81: ES-MS for compound **7m**; Figure S82: ^{1}H NMR Spectrum of **7n**; Figure S83: ^{13}C NMR Spectrum of **7n**; Figure S84: ES-MS for compound **7n**.

Author Contributions: Conceptualization, X.W., B.J. and H.Y.; methodology, X.W., B.J., Y.H., T.W., Z.S., Y.T. and H.Y.; software, Z.S.; validation, X.W., B.J., Y.H., T.W., Z.S., Y.T. and H.Y.; formal analysis, X.W., B.J. and H.Y.; investigation, H.Y.; resources, H.Y.; data curation, X.W., B.J. and H.Y.; writing—original draft preparation, X.W.; writing—review and editing, H.Y.; visualization, Z.S.; supervision, H.Y.; project administration, H.Y.; funding acquisition, H.Y. All authors have read and agreed to the published version of the manuscript.

Institutional Review Board Statement: Not applicable.

Informed Consent Statement: Not applicable.

References

1. Yan, X.; Schouls, L.M.; Pluister, G.N.; Tao, X.; Yu, X.; Yin, J.; Song, Y.; Hu, S.; Luo, F.; Hu, W.; et al. The population structure of *Staphylococcus aureus* in China and Europe assessed by multiple-locus variable number tandem repeat analysis; clues to geographical origins of emergence and dissemination. *Clin. Microbiol. Infect.* **2016**, *22*, 60.e1–60.e8. [CrossRef] [PubMed]
2. Zaman, S.B.; Hussain, M.A.; Nye, R.; Mehta, V.; Mamun, K.T.; Hossain, N. A Review on Antibiotic Resistance: Alarm Bells are Ringing. *Cureus* **2017**, *9*, e1403. [CrossRef]
3. Parrino, B.; Schillaci, D.; Carnevale, I.; Giovannetti, E.; Diana, P.; Cirrincione, G.; Cascioferro, S. Synthetic small molecules as anti-biofilm agents in the struggle against antibiotic resistance. *Eur. J. Med. Chem.* **2019**, *161*, 154–178. [CrossRef]
4. Costerton, J.W.; Stewart, P.S.; Greenberg, E.P. Bacterial Biofilms: A Common Cause of Persistent Infections. *Science* **1999**, *284*, 1318–1322. [CrossRef] [PubMed]
5. Liang, J.; Sun, D.; Yang, Y.; Li, M.; Li, H.; Chen, L. Discovery of metal-based complexes as promising antimicrobial agents. *Eur. J. Med. Chem.* **2021**, *224*, 113696. [CrossRef] [PubMed]
6. Ling, H.; Lou, X.; Luo, Q.; He, Z.; Sun, M.; Sun, J. Recent advances in bacteriophage-based therapeutics: Insight into the post-antibiotic era. *Acta Pharm. Sin. B* **2022**, *12*, 4348–4364. [CrossRef]
7. Pisoschi, A.M.; Pop, A.; Cimpeanu, C.; Turcuş, V.; Predoi, G.; Iordache, F. Nanoencapsulation techniques for compounds and products with antioxidant and antimicrobial activity—A critical view. *Eur. J. Med. Chem.* **2018**, *157*, 1326–1345. [CrossRef]
8. Wang, Y.; Lv, Q.; Chen, Y.; Xu, L.; Feng, M.; Xiong, Z.; Li, J.; Ren, J.; Liu, J.; Liu, B. Bilayer hydrogel dressing with lysozyme-enhanced photothermal therapy for biofilm eradication and accelerated chronic wound repair. *Acta Pharm. Sin. B* **2022**, *13*, 284–297. [CrossRef]
9. Malla, T.R.; Brewitz, L.; Muntean, D.G.; Aslam, H.; Owen, C.D.; Salah, E.; Tumber, A.; Lukacik, P.; Strain-Damerell, C.; Mikolajek, H.; et al. Penicillin Derivatives Inhibit the SARS-CoV-2 Main Protease by Reaction with Its Nucleophilic Cysteine. *J. Med. Chem.* **2022**, *65*, 7682–7696. [CrossRef]
10. Naclerio, G.A.; Abutaleb, N.S.; Onyedibe, K.I.; Karanja, C.; Eldesouky, H.E.; Liang, H.W.; Dieterly, A.; Aryal, U.K.; Lyle, T.; Seleem, M.N.; et al. Mechanistic Studies and In Vivo Efficacy of an Oxadiazole-Containing Antibiotic. *J. Med. Chem.* **2022**, *65*, 6612–6630. [CrossRef]
11. Xie, Y.P.; Sangaraiah, N.; Meng, J.P.; Zhou, C.H. Unique Carbazole-Oxadiazole Derivatives as New Potential Antibiotics for Combating Gram-Positive and -Negative Bacteria. *J. Med. Chem.* **2022**, *65*, 6171–6190. [CrossRef] [PubMed]
12. Zurenko, G.E.; Yagi, B.H.; Schaadt, R.D.; Allison, J.W.; Kilburn, J.O.; Glickman, S.E.; Hutchinson, D.K.; Barbachyn, M.R.; Brickner, S.J. In vitro activities of U-100592 and U-100766, novel oxazolidinone antibacterial agents. *Antimicrob. Agents Chemother.* **1996**, *40*, 839–845. [CrossRef] [PubMed]
13. Lei, H.; Jiang, Y.; Wang, D.; Gong, P.; Li, Y.; Dong, Y.; Dong, M. In vitro activity of novel oxazolidinone analogs and 13 conventional antimicrobial agents against clinical isolates of *Staphylococcus aureus* in Beijing, China. *Jpn. J. Infect. Dis.* **2014**, *67*, 402–404. [CrossRef]
14. Lin, A.H.; Murray, R.W.; Vidmar, T.J.; Marotti, K.R. The oxazolidinone eperezolid binds to the 50S ribosomal subunit and competes with binding of chloramphenicol and lincomycin. *Antimicrob. Agents Chemother.* **1997**, *41*, 2127–2131. [CrossRef]
15. Swaney, S.M.; Aoki, H.; Ganoza, M.C.; Shinabarger, D.L. The oxazolidinone linezolid inhibits initiation of protein synthesis in bacteria. *Antimicrob. Agents Chemother.* **1998**, *42*, 3251–3255. [CrossRef] [PubMed]
16. Zhou, C.C.; Swaney, S.M.; Shinabarger, D.L.; Stockman, B.J. 1H nuclear magnetic resonance study of oxazolidinone binding to bacterial ribosomes. *Antimicrob. Agents Chemother.* **2002**, *46*, 625–629. [CrossRef]
17. Foti, C.; Piperno, A.; Scala, A.; Giuffrè, O. Oxazolidinone Antibiotics: Chemical, Biological and Analytical Aspects. *Molecules* **2021**, *26*, 4280. [CrossRef]
18. Pandit, N.; Singla, R.K.; Shrivastava, B. Current updates on oxazolidinone and its significance. *Int. J. Med. Chem.* **2012**, *2012*, 159285. [CrossRef]
19. Yuan, S.; Shen, D.D.; Bai, Y.R.; Zhang, M.; Zhou, T.; Sun, C.; Zhou, L.; Wang, S.Q.; Liu, H.M. Oxazolidinone: A promising scaffold for the development of antibacterial drugs. *Eur. J. Med. Chem.* **2023**, *250*, 115239. [CrossRef]
20. Vinh, D.C.; Rubinstein, E. Linezolid: A review of safety and tolerability. *J. Infect.* **2009**, *59* (Suppl. S1), S59–S74. [CrossRef]
21. Bai, P.-Y.; Qin, S.-S.; Chu, W.-C.; Yang, Y.; Cui, D.-Y.; Hua, Y.-G.; Yang, Q.-Q.; Zhang, E. Synthesis and antibacterial bioactivies of cationic deacetyl linezolid amphiphiles. *Eur. J. Med. Chem.* **2018**, *155*, 925–945. [CrossRef]
22. De Rosa, M.; Zanfardino, A.; Notomista, E.; Wichelhaus, T.A.; Saturnino, C.; Varcamonti, M.; Soriente, A. Novel promising linezolid analogues: Rational design, synthesis and biological evaluation. *Eur. J. Med. Chem.* **2013**, *69*, 779–785. [CrossRef] [PubMed]

23. Fortuna, C.G.; Bonaccorso, C.; Bulbarelli, A.; Caltabiano, G.; Rizzi, L.; Goracci, L.; Musumarra, G.; Pace, A.; Palumbo Piccionello, A.; Guarcello, A.; et al. New linezolid-like 1,2,4-oxadiazoles active against Gram-positive multiresistant pathogens. *Eur. J. Med. Chem.* **2013**, *65*, 533–545. [CrossRef]

24. Gadekar, P.K.; Roychowdhury, A.; Kharkar, P.S.; Khedkar, V.M.; Arkile, M.; Manek, H.; Sarkar, D.; Sharma, R.; Vijayakumar, V.; Sarveswari, S. Design, synthesis and biological evaluation of novel azaspiro analogs of linezolid as antibacterial and antitubercular agents. *Eur. J. Med. Chem.* **2016**, *122*, 475–487. [CrossRef]

25. Naresh, A.; Venkateswara Rao, M.; Kotapalli, S.S.; Ummanni, R.; Venkateswara Rao, B. Oxazolidinone derivatives: Cytoxazone-linezolid hybrids induces apoptosis and senescence in DU145 prostate cancer cells. *Eur. J. Med. Chem.* **2014**, *80*, 295–307. [CrossRef] [PubMed]

26. Palumbo Piccionello, A.; Musumeci, R.; Cocuzza, C.; Fortuna, C.G.; Guarcello, A.; Pierro, P.; Pace, A. Synthesis and preliminary antibacterial evaluation of Linezolid-like 1,2,4-oxadiazole derivatives. *Eur. J. Med. Chem.* **2012**, *50*, 441–448. [CrossRef]

27. Wei, H.; Mao, F.; Ni, S.; Chen, F.; Li, B.; Qiu, X.; Hu, L.; Wang, M.; Zheng, X.; Zhu, J.; et al. Discovery of novel piperonyl derivatives as diapophytoene desaturase inhibitors for the treatment of methicillin-, vancomycin- and linezolid-resistant *Staphylococcus aureus* infections. *Eur. J. Med. Chem.* **2018**, *145*, 235–251. [CrossRef]

28. Wu, Y.; Ding, X.; Ding, L.; Zhang, Y.; Cui, L.; Sun, L.; Li, W.; Wang, D.; Zhao, Y. Synthesis and antibacterial activity evaluation of novel biaryloxazolidinone analogues containing a hydrazone moiety as promising antibacterial agents. *Eur. J. Med. Chem.* **2018**, *158*, 247–258. [CrossRef] [PubMed]

29. Wu, Y.; Ding, X.; Yang, Y.; Li, Y.; Qi, Y.; Hu, F.; Qin, M.; Liu, Y.; Sun, L.; Zhao, Y. Optimization of biaryloxazolidinone as promising antibacterial agents against antibiotic-susceptible and antibiotic-resistant gram-positive bacteria. *Eur. J. Med. Chem.* **2020**, *185*, 111781. [CrossRef]

30. Jin, B.; Chen, J.Y.; Sheng, Z.L.; Sun, M.Q.; Yang, H.L. Synthesis, Antibacterial and Anthelmintic Activity of Novel 3-(3-Pyridyl)-oxazolidinone-5-methyl Ester Derivatives. *Molecules* **2022**, *27*, 1103. [CrossRef]

31. Jin, B.; Wang, T.; Chen, J.Y.; Liu, X.Q.; Zhang, Y.X.; Zhang, X.Y.; Sheng, Z.L.; Yang, H.L. Synthesis and Biological Evaluation of 3-(Pyridine-3-yl)-2-Oxazolidinone Derivatives as Antibacterial Agents. *Front. Chem.* **2022**, *10*, 949813. [CrossRef]

32. Yang, H.-l.; Jin, B.; Chen, J.-q.; Sheng, Z.-l. Synthesis and Biological Activity of Pyridinyl-4,5-2H-isoxazole Heterocyclic Derivatives. *Fine Chem.* **2019**, *36*, 487.

33. Yang, H.-L.; Xu, G.-X.; Bao, M.-Y.; Zhang, D.-P.; Li, Z.-W.; Pei, Y.-Z. Design and Synthesis of Pyridinylisoxazoles and Their Anticancer Activities. *Chem. J. Chin. Univ.* **2014**, *35*, 2584.

34. Yang, H.-l.; Xu, G.-x.; Pei, Y.-z. Synthesis, preliminary structure-activity relationships and biological evaluation of pyridinyl-4,5-2H-isoxazole derivatives as potent antitumor agents. *Chem. Res. Chin. Univ.* **2017**, *33*, 61–69. [CrossRef]

35. Elattar, K.M.; Mert, B.D.; Monier, M.; El-Mekabaty, A. Advances in the chemical and biological diversity of heterocyclic systems incorporating pyrimido[1,6-a]pyrimidine and pyrimido[1,6-c]pyrimidine scaffolds. *RSC Adv.* **2020**, *10*, 15461–15492. [CrossRef] [PubMed]

36. Albratty, M.; Alhazmi, H.A. Novel pyridine and pyrimidine derivatives as promising anticancer agents: A review. *Arab. J. Chem.* **2022**, *15*, 103846. [CrossRef]

37. Tao, Y.; Chen, J.X.; Fu, Y.; Chen, K.; Luo, Y. Exploratory Process Development and Kilogram-Scale Synthesis of a Novel Oxazolidinone Antibacterial Candidate. *Org. Process Res. Dev.* **2014**, *18*, 511–519. [CrossRef]

38. Phillips, O.A.; D'Silva, R.; Bahta, T.O.; Sharaf, L.H.; Udo, E.E.; Benov, L.; Eric Walters, D. Synthesis and biological evaluation of novel 5-(hydroxamic acid)methyl oxazolidinone derivatives. *Eur. J. Med. Chem.* **2015**, *106*, 120–131. [CrossRef]

39. Wang, Y.; Shen, J.K.; Schroeder, S.J. Nucleotide Dynamics at the A-Site Cleft in the Peptidyltransferase Center of H. marismortui 50S Ribosomal Subunits. *J. Phys. Chem. Lett.* **2012**, *3*, 1007–1010. [CrossRef]

40. Kotb, A.; Abutaleb, N.S.; Seleem, M.A.; Hagras, M.; Mohammad, H.; Bayoumi, A.; Ghiaty, A.; Seleem, M.N.; Mayhoub, A.S. Phenylthiazoles with tert-Butyl side chain: Metabolically stable with anti-biofilm activity. *Eur. J. Med. Chem.* **2018**, *151*, 110–120. [CrossRef]

41. Ding, R.; Wang, X.; Fu, J.; Chang, Y.; Li, Y.; Liu, Y.; Liu, Y.; Ma, J.; Hu, J. Design, synthesis and antibacterial activity of novel pleuromutilin derivatives with thieno[2,3-d]pyrimidine substitution. *Eur. J. Med. Chem.* **2022**, *237*, 114398. [CrossRef] [PubMed]

42. Wiegand, I.; Hilpert, K.; Hancock, R.E. Agar and broth dilution methods to determine the minimal inhibitory concentration (MIC) of antimicrobial substances. *Nat. Protoc.* **2008**, *3*, 163–175. [CrossRef] [PubMed]

43. Ippolito, J.A.; Kanyo, Z.F.; Wang, D.; Franceschi, F.J.; Moore, P.B.; Steitz, T.A.; Duffy, E.M. Crystal Structure of the Oxazolidinone Antibiotic Linezolid Bound to the 50S Ribosomal Subunit. *J. Med. Chem.* **2008**, *51*, 3353–3356. [CrossRef] [PubMed]

44. Noolvi, M.N.; Patel, H.M.; Kamboj, S.; Kaur, A.; Mann, V. 2,6-Disubstituted imidazo[2,1-b][1,3,4]thiadiazoles: Search for anticancer agents. *Eur. J. Med. Chem.* **2012**, *56*, 56–69. [CrossRef]

45. Vaarla, K.; Kesharwani, R.K.; Santosh, K.; Vedula, R.R.; Kotamraju, S.; Toopurani, M.K. Synthesis, biological activity evaluation and molecular docking studies of novel coumarin substituted thiazolyl-3-aryl-pyrazole-4-carbaldehydes. *Bioorg. Med. Chem. Lett.* **2015**, *25*, 5797–5803. [CrossRef]